



## Treatment of inclined EAS data from surface arrays and GZK prediction

J. N. CAPDEVIELLE<sup>1</sup>, F. COHEN<sup>2</sup>, B. SZABELSKA<sup>3</sup>, J. SZABELSKI<sup>3</sup>

<sup>1</sup>*Astroparticules et Cosmologie, Univ. de Paris 7, 10 rue Alice Domont et Leonie Duquet, 75205 Paris, France*

<sup>2</sup>*Institute for Cosmic Ray Research, University of Tokyo, Japan*

<sup>3</sup>*The Andrzej Soltan Institute for Nuclear Studies, Cosmic Ray Laboratory 90-950 Lodz 1, POBox 447, Poland*

capdev@apc.univ-paris7.fr

**Abstract:** Beyond  $5 \cdot 10^{19}$  eV a complex situation happens for the "attenuation" in inclined showers. When the depth of maximum is close to the experimental plane, for a given primary energy, the density in the inclined shower at 600 or 1000 m exceeds the corresponding vertical density for the same energy, sometimes by 10% between  $10^\circ - 30^\circ$ . This is a simple consequence of the 3D e.m. cascade theory (larger densities at larger distances for older profiles of the lateral distributions). An algorithm is proposed to restore the correct primary energy and amend the previous intensity overestimated for 60 – 70% of the solid angle inside  $45^\circ$ . The similar behaviour of muons and converted photons have an additive contribution to this process. The amended AGASA data would also agree with the GZK prediction.

### Introduction

We have previously emphasized [3, 4, 6] that the primary energy in the surface array was mainly overestimated by reason of an inappropriate conversion of the energy estimation, i.e. the density,  $S_{600}(\Theta)$  to the vertical density  $S_{600}(0^\circ)$ , for giant inclined showers. Recently, the group of AGASA reduced the intensity of ultra-high energy [5] and started a new calibration of the raw data.

The important discrepancy in the determination of the primary energy spectrum above  $10^{19}$  eV was underlined 6 years ago [1] and the convergence to GZK behaviour was underlined by the recent compilation of HiRES 1, 2 and HiRES stereo [2].

### Simulations and estimators

Simulations with CORSIKA have been performed for gammas, protons and iron nuclei as primary particles for 6 energies and in most cases for 8 different zenith angles. In each combinations of primary particle, energy and zenith angle there were 40 EAS simulated [9]. Presented here values are

average numbers from 40 EAS (longitudinal developments can be found in [6]).

The Fig. 1 exhibits the relative dependence of the electron densities (at 600 m) on zenith angle. The solid line (bottom) represents the AGASA conversion of particle density at 600 m from zenith angle  $\Theta$  to the corresponding value for vertical shower (formula 1). This conversion inferred by fitting the attenuation of  $S_{600}$  [10] is represented by:

$$S_{600}(\Theta) = S_{600}(0) \times \exp\left(-\frac{t_0}{\Lambda_1}(\sec(\Theta) - 1) - \frac{t_0}{\Lambda_2}(\sec(\Theta) - 1)^2\right) \quad (1)$$

with  $\Lambda_2 = 594 \text{ gcm}^{-2}$  and  $\Lambda_1 = 500 \text{ gcm}^{-2}$ . The simulations at ultra high energy contradict the classical absorption behaviour of relation 1 (fig.1): the density increases progressively in function of the primary energy versus  $\sec(\Theta)$  reaching a maximum between  $10-20^\circ$  and then decreases with zenith angle for primary protons ( $E_0 = 10^9, 5 \cdot 10^9, 10^{10}, 5 \cdot 10^{10}, 10^{11} \text{ GeV}$ ).

A similar increase of the estimator density appears in the calculations performed with AIRES [12], plotted versus the distance between the experimental plane and the maximum depth. Such situation

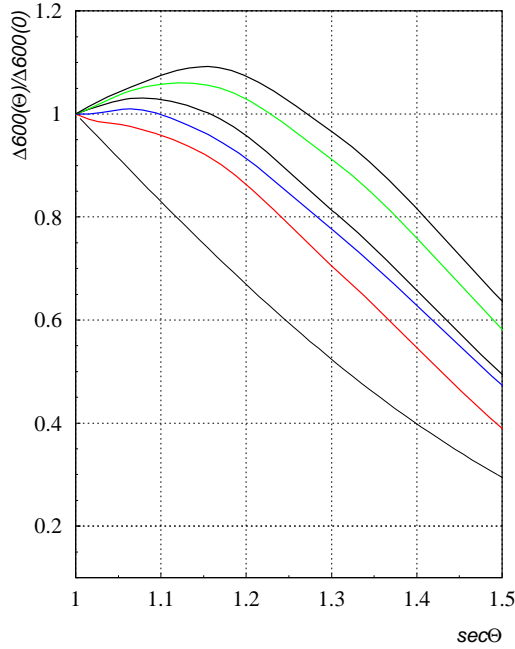


Figure 1: Dependence  $\frac{(S_{600}(\Theta))}{(S_{600}(0))}$  versus  $sec(\theta)$  for protons with  $E_0 = 10^9, 5.10^9, 10^{10}, 5.10^{10}, 10^{11} GeV$  (from the bottom to the top) respectively for models of high multiplicity (bottom curve for formula 1).

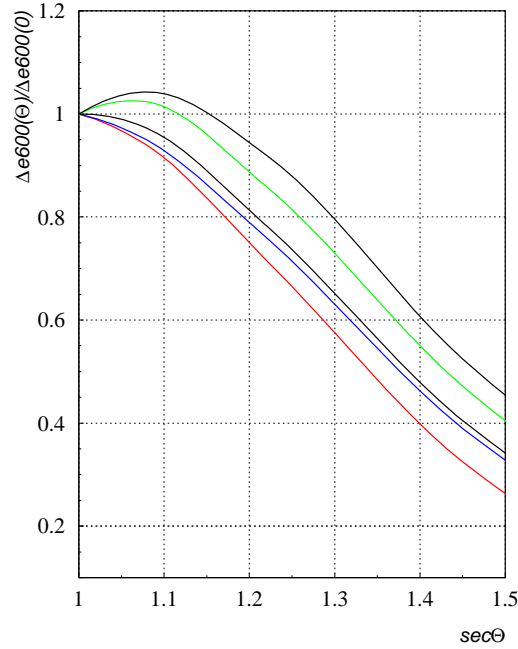


Figure 2: Dependence  $\frac{(S_{600}(\Theta))}{(S_{600}(0))}$  versus  $sec(\theta)$  for protons with  $E_0 = 10^9, 5.10^9, 10^{10}, 5.10^{10}, 10^{11} GeV$  (from the bottom to the top) respectively for models of low multiplicity .

in the case of AUGER corresponds to a maximum depth of the longitudinal development at about one electron radiation length (for  $E_0 = 10^{11}$  GeV) above the experimental array (a similar situation in AGASA would be obtained with a model of modest multiplicity such as HDPM). For a model with large multiplicity, such as QGSJET2, the same maximum is near 3 radiation lengths above AGASA and the total discrepancy is slightly reduced on fig. 2 (respective depths  $t_o$  of  $860 \text{ gcm}^{-2}$  for AUGER and  $920 \text{ gcm}^{-2}$  for AGASA).

To illustrate the discrepancies between showers induced by iron primaries instead of protons, we compare in Fig.3 the behaviour of the densities versus zenith angle at  $10^{11}$  GeV. The contribution of photons and muons is presented on the lower part of Fig.4 and the role of converted photons is also important for AUGER.

### Analytical description with distorted gaussian function

This typical behaviour can be described analytically by the so called distorted gaussian function:

$$f(l) = A \times \exp\left(\frac{k}{8} - \frac{s\delta}{2} - \frac{1}{4}(2+k)\delta^2 + \frac{1}{6}s\delta^3 + \frac{1}{24}k\delta^4\right) \quad (2)$$

where:  $l = sec(\Theta)$ ,  $\delta = (l - \langle l \rangle) / \sigma$

$$\sigma^2 = \langle l^2 \rangle - \langle l \rangle^2$$

$$s = \langle (l - \langle l \rangle)^3 \rangle / \sigma^3 \text{ skewness,}$$

$$k = \langle (l - \langle l \rangle)^4 \rangle / \sigma^4 \text{ kurtosis.}$$

Values of parameters in formula 2 are summarized in the Table 5 for the 1st class of interaction models (table for other models in [6]).

The dependence shown in Fig.1 is a general consequence of the electromagnetic cascade theory. The discrepancy with "AGASA absorption" is slightly reduced (Fig.2) in the case of iron primaries as the

Figure 5: Coefficients  $A$ ,  $\langle l \rangle$ ,  $\sigma$ ,  $s$  and  $k$

$E_0$ (eV)	$A$	$\langle l \rangle$	$\sigma$	$s$	$k$
$10^{20}$	1.1	1.159	0.339	$0.143 \cdot 10^{-5}$	$0.832 \cdot 10^{-1}$
$5 \cdot 10^{19}$	1.06	1.146	0.341	$0.244 \cdot 10^{-5}$	0.158
$10^{19}$	1.032	1.090	0.345	$0.300 \cdot 10^{-4}$	0.104
$5 \cdot 10^{18}$	1.011	1.029	0.384	$0.242 \cdot 10^{-6}$	$0.191 \cdot 10^{-2}$
$10^{18}$	1.0	0.998	0.368	$0.179 \cdot 10^{-5}$	$0.203 \cdot 10^{-1}$

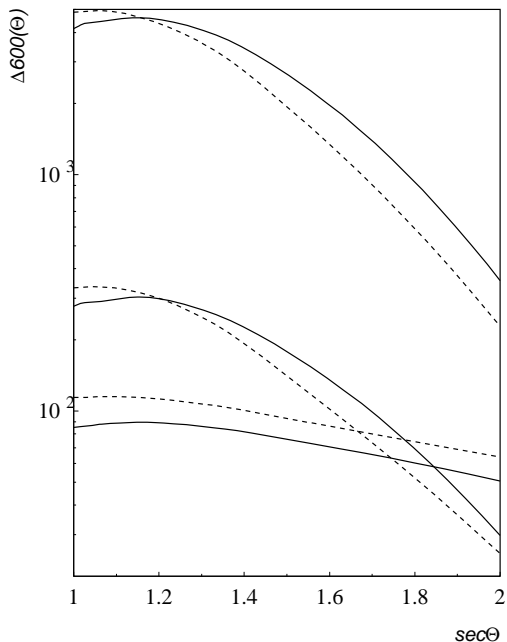


Figure 3: Densities versus  $\Theta$  for proton (solid lines) and iron primaries (dashed lines) at  $10^{11}$  GeV (from top:  $\gamma$ 's, electrons and muons).

maximum is higher in the atmosphere than for protons. Furthermore, the LPM effect concerns more the photoelectronic cascades of larger energies in proton showers.

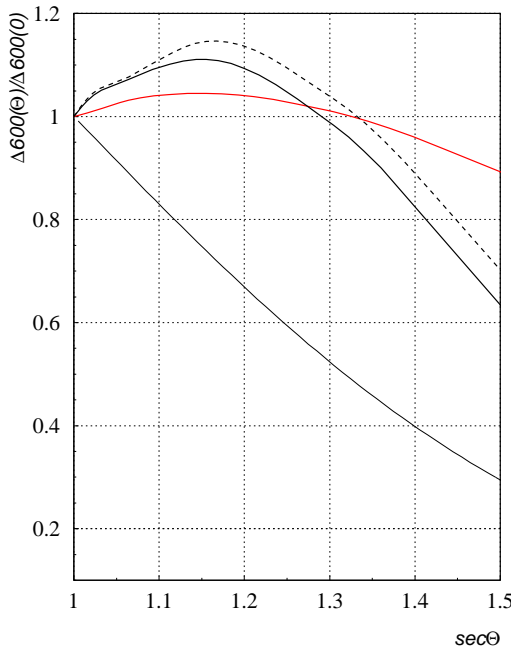


Figure 4: Dependence  $\frac{\Delta_{600}(\Theta)}{\Delta_{600}(0)}$  versus  $sec(\theta)$  for proton primaries of  $10^{11}$  GeV. From the top:  $\gamma$ 's above 20 MeV (dashed line),  $\gamma$ 's above 2 MeV (solid line), muons above 250 MeV and absorption as formula 1.

### Induced divergence in the primary spectrum

To understand how the results of AGASA could be amended, we have simulated  $2 \cdot 10^8$  EAS above  $10^{18}$  eV with an  $E^{-3}$  spectrum and examined the reconstruction.

Both primary energy and zenith angle are generated. The vertical density at 600 m from the axis is first sampled from the distribution derived from our CORSIKA data bank and transformed to density  $S_{600}(\Theta)$  by interpolation on the primary energy in relation 2. This density is then converted to  $S_{600}(0)$  following the treatment of AGASA through the formula 1 for zenith angle  $\Theta$ . In the last step, the primary energy  $E_0$  (in eV) is recovered with the conversion of AGASA [5]:

$$E_0 = 1.96 \cdot 10^{19} \left( \frac{S_{600}(0)}{100} \right)^{1.02} \quad (3)$$

For both configurations of Fig.1 and Fig.2, the divergence at ultra high energy introduced artificially in the primary spectrum was ascertained [6].

Implementing in the generation the spectrum described by 3 power laws introduced by Bergman(2003) (exponent  $\gamma = 3.12, 2.86, 5$  respectively for  $\text{Log}(E_0) \leq 18.47, 19.79$  and  $\geq 19.79$ ), we ascertain the energy overestimation also generated in proportion to the discrepancy between AGASA and HIREs(Fig.6).

## Conclusions

The present approach points out a better consistency between the spectra obtained by surface arrays and Hires measurements. The earliest energy overestimation by the AGASA treatment of inclined showers was increasing artificially the primary index in a proportion rising with the primary energy: the AGASA spectrum can be now amended by an adequate procedure determining the energy of inclined showers. A general convergence towards the GZK prediction can be expected.

## References

- [1] R. Sommers, rap.pap., 27th ICRC, Hamburg, 2001
- [2] P. Sokolsky, inv. talk, XIV ISVHECRI, Weihai, 2006
- [3] J.N. Capdevielle and F. Cohen, 29<sup>th</sup> ICRC, Pune, 7, 59-62 (2005)
- [4] J.N. Capdevielle and F. Cohen, J.Phys.G 31, 1413-1419 (2005)
- [5] K. Shinozaki, inv. talk, XIV ISVHECRI, Weihai, 2006
- [6] J.N. Capdevielle, F.Cohen, B. Szabelska, J. Szabelski, Proc. 20<sup>th</sup> ECRS, Lisbon, 2006
- [7] D. Heck, J. Knapp, J.N. Capdevielle, G. Schatz and T. Thouw FZK A report-6019 ed. FZK. The CORSIKA Air Shower Simulation Program, Karlsruhe (1998)
- [8] J.N. Capdevielle and F. Cohen, J.Phys. G, Nucl. Part. Phys., 31, 507-524 (2005)
- [9] F. Cohen, Ph. D. thesis, Univ. Paris XI (2003)
- [10] S. Yoshida et al., J. Phys. G 20, 651-664 (1994)
- [11] D. Bergman et al., 28<sup>th</sup> ICRC, Tsukuba, 1, 299 (2003)
- [12] Aaron D. Chou, Phys. Rev. D, 74, 103001(2006)

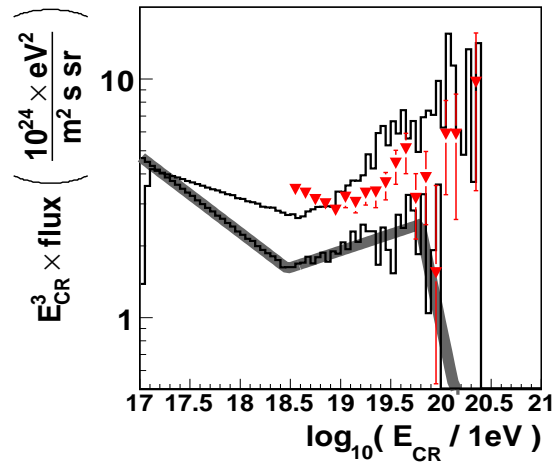


Figure 6: Bergman's spectrum (grey band) and AGASA spectrum [2] represented by triangles. For the clarity of the graph, HIREs spectrum is not plotted here as approximately superimposed on the Bergman's spectrum. The upper histogram represents the excess generated with the assumptions of Table 5 and further reconstruction of the primary energy by AGASA method.